Supplementary Figures

Supplementary Figure 1

A

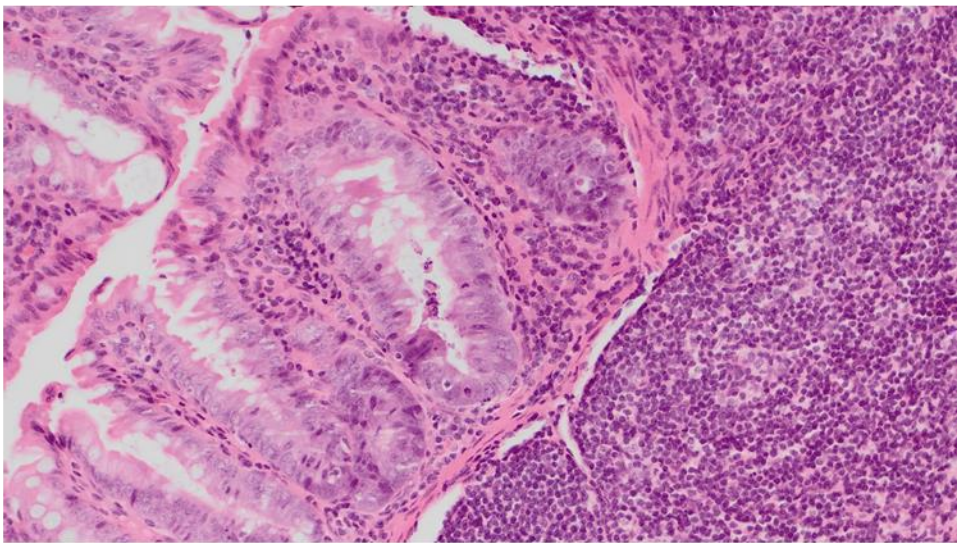

B

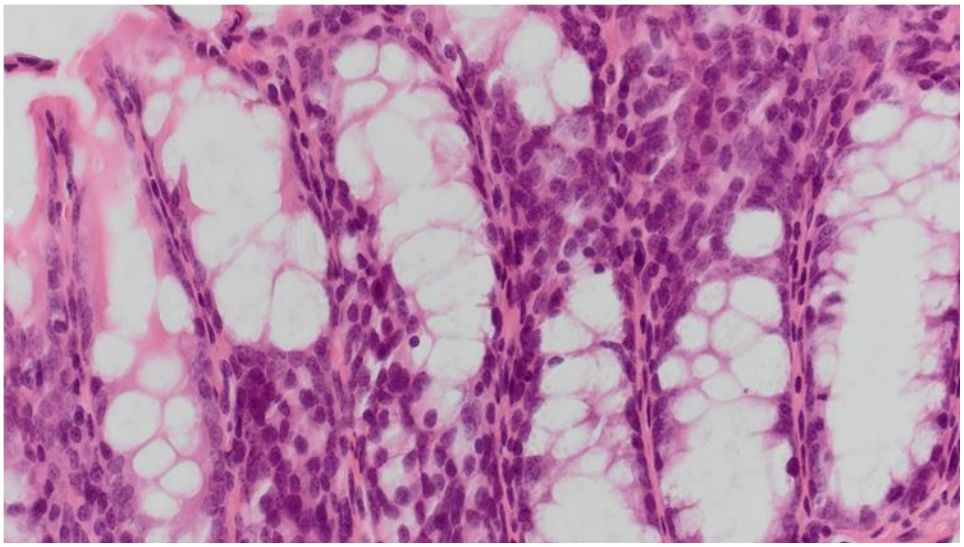

Supplementary Figure 1. Further histological evidence showing marked crypt apoptosis and increased lymphocyte infiltration in CPI-induced colitis mice

(A) Marked crypt apoptosis and (B) lymphocyte infiltration of the lamina propria in mice treated with combination anti-CTLA/anti-PD-1 therapy and FMT.

Supplementary Figure 2

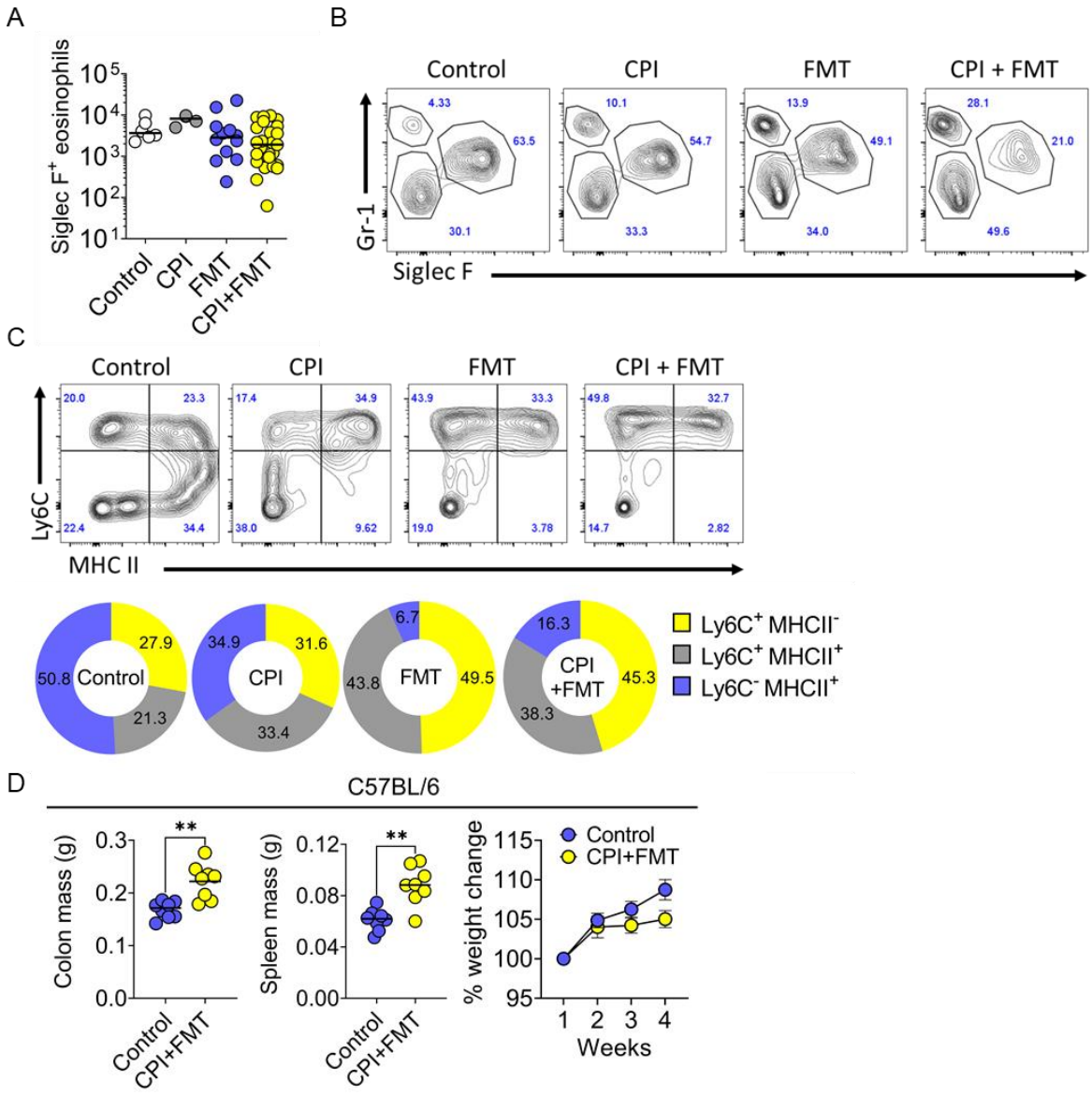

Supplementary Figure 2. The intestinal microbiota regulates susceptibility to immune checkpoint inhibitor-induced colitis

(A) Number of Siglec F^+ eosinophils and (B) representative flow cytometry contour plots showing neutrophils (Gr-1^+ SiglecF^-) and eosinophils (Gr-1^- SiglecF^+) (pre-gated on live $CD45^+$ $CD11b^+$) in the lamina propria of the colon in wildtype Balb/C mice without treatment (control, n=6), treatment with combination anti-CTLA4/anti-PD-1 (CPI, n=3), treatment with faecal microbiota (FMT, n=13) and mice treated with both CPI and FMT (n=54). (C)

Representative flow cytometry contour plots and the overall ratio of infiltrating monocytes ($Ly6C^+$ $MHCII^-$), transitioning monocytes ($Ly6C^+$ $MHCII^+$) and resident macrophages ($Ly6C^-$ $MHCII^+$) (pre-gated on live $CD45^+$ $CD11b^+$ $Gr\text{-}1^-$ $SiglecF^-$) present in the lamina propria of wildtype control mice (n=6), mice with only CPI treatment (n=6), mice given only FMT (n=6) and mice treated with both CPI and FMT (n=6). (D) Colon mass, spleen mass and the percentage weight change between untreated C56BL/6 mice (n=8) and C56BL/6 mice treated with both CPI and FMT (n=8). ** $P < 0.005$ with two-sided Mann-Whitney U Test.

Supplementary Figure 3

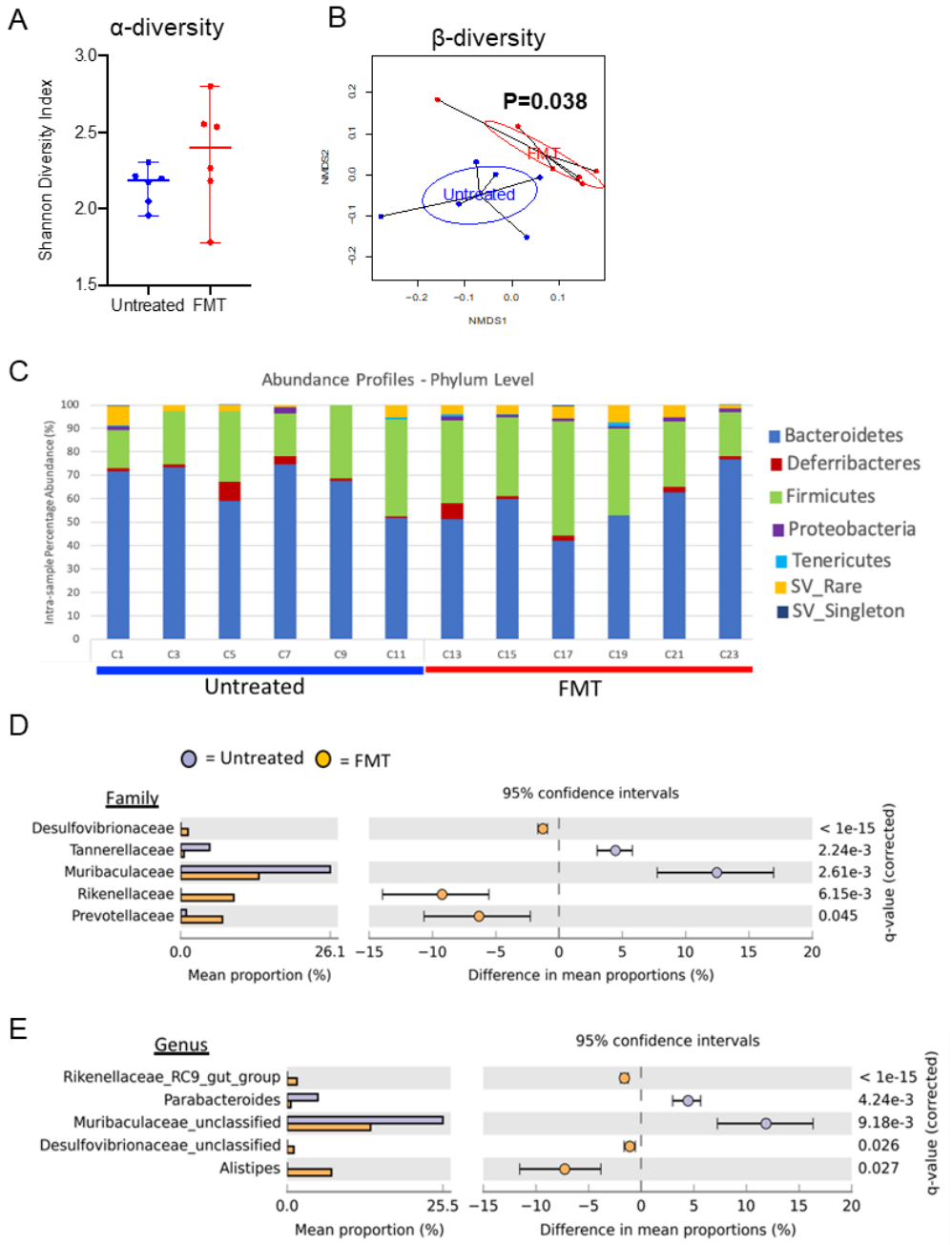

Supplementary Figure 3: Faecal microbiota transplantation alters the community composition of the intestinal microbiota

(A) Alpha diversity (Shannon diversity index) of the microbiota between untreated control Balb/C WT (n=6) and Balb/C WT treated with FMT (n=6). (B) Non-metric dimensional scaling plot showing the beta diversity of the microbiota from untreated control Balb/C WT (n=6) and Balb/C WT treated with FMT (n=6). (C) Phylum level relative abundance profiles for untreated

control Balb/C WT (n=6) and Balb/C WT treated with FMT (n=6). (D) Extended error bar plot, with bacterial family changes statistically assessed by White's non-parametric t-test with Benjamini-Hochberg correction, using threshold of differences between mean proportions >1% between untreated control Balb/C WT (n=6) and Balb/C WT treated with FMT (n=6). (E) Extended error bar plot, with bacterial genus statistically significant changes measured by White's non-parametric t-test with Benjamini-Hochberg correction, using threshold of differences between mean proportions >1% between untreated control Balb/C WT (n=6) and Balb/C WT treated with FMT (n=6).

Supplementary Figure 4

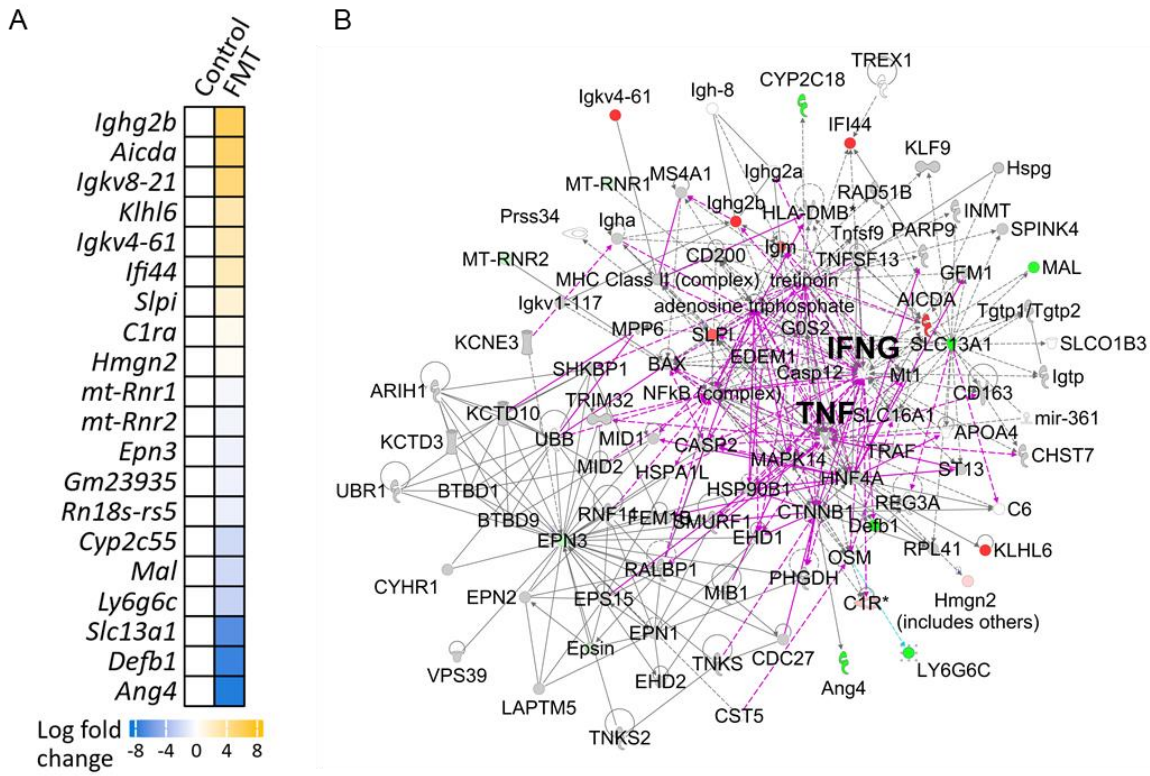

Supplementary Figure 4: Gene expression changes in the colon of WT mice following FMT

RNA was extracted from the distal colon of WT mice following gavage with a pro-inflammatory microbiota, harvested from TRUC mice and RNA sequencing performed. (A) DEGs (FDR<0.05) in the colon of WT mice following FMT (n=3) in comparison with control mice (n=4). (B) The only 3 mechanistic networks associated with the gene expression changes occurring in FMT recipients in comparison with control mice were merged to form a single network (IPA, QIAGEN).

Supplementary Figure 5

A

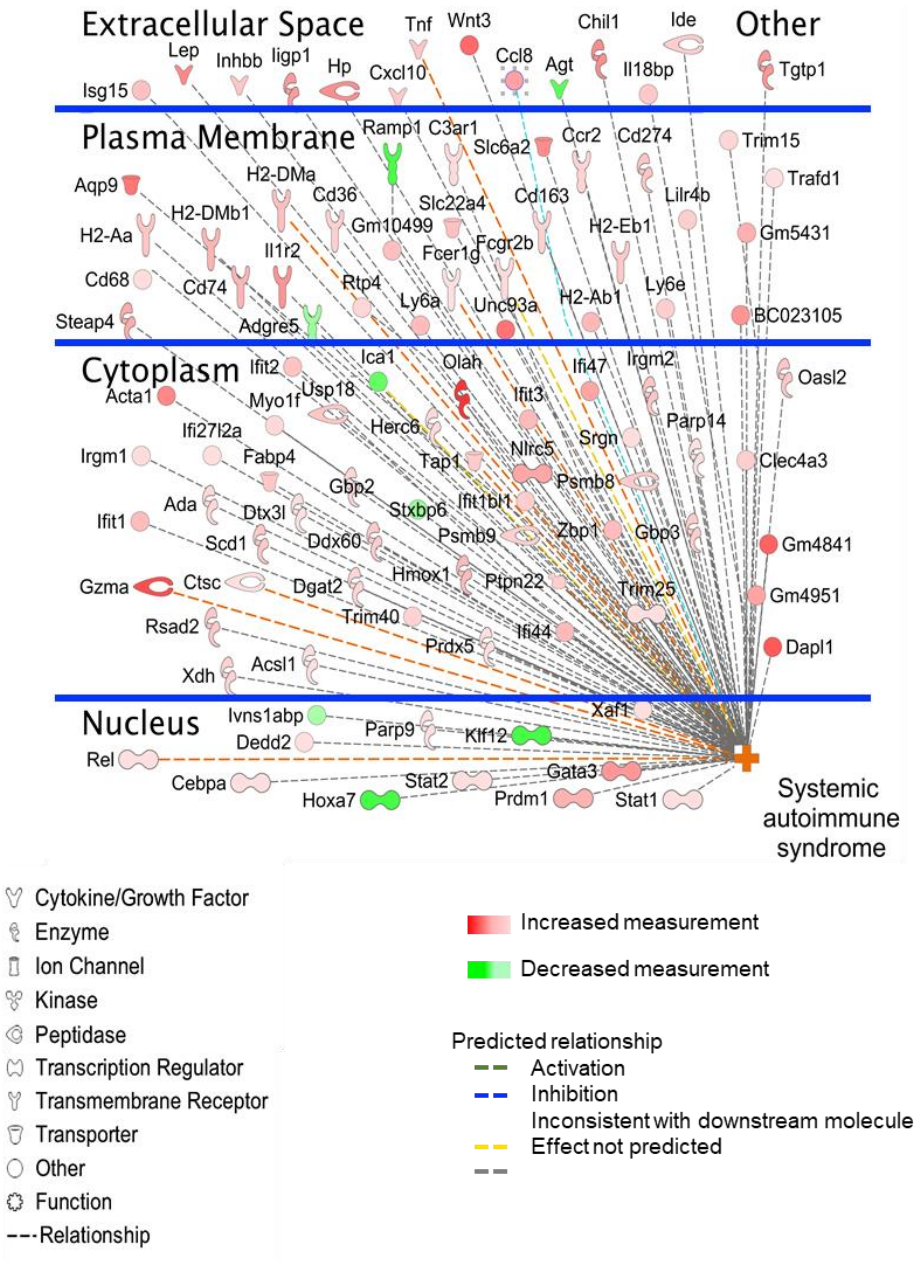

Supplementary Figure 5: Causal network analysis of the most enriched pathway identified in the colon of WT mice following FMT+CPI

(A) Network analysis showing the causal networks associated with the gene expression changes occurring in mice treated with FMT+CPI in comparison to control mice and merged to show one single network.

Supplementary Figure 6

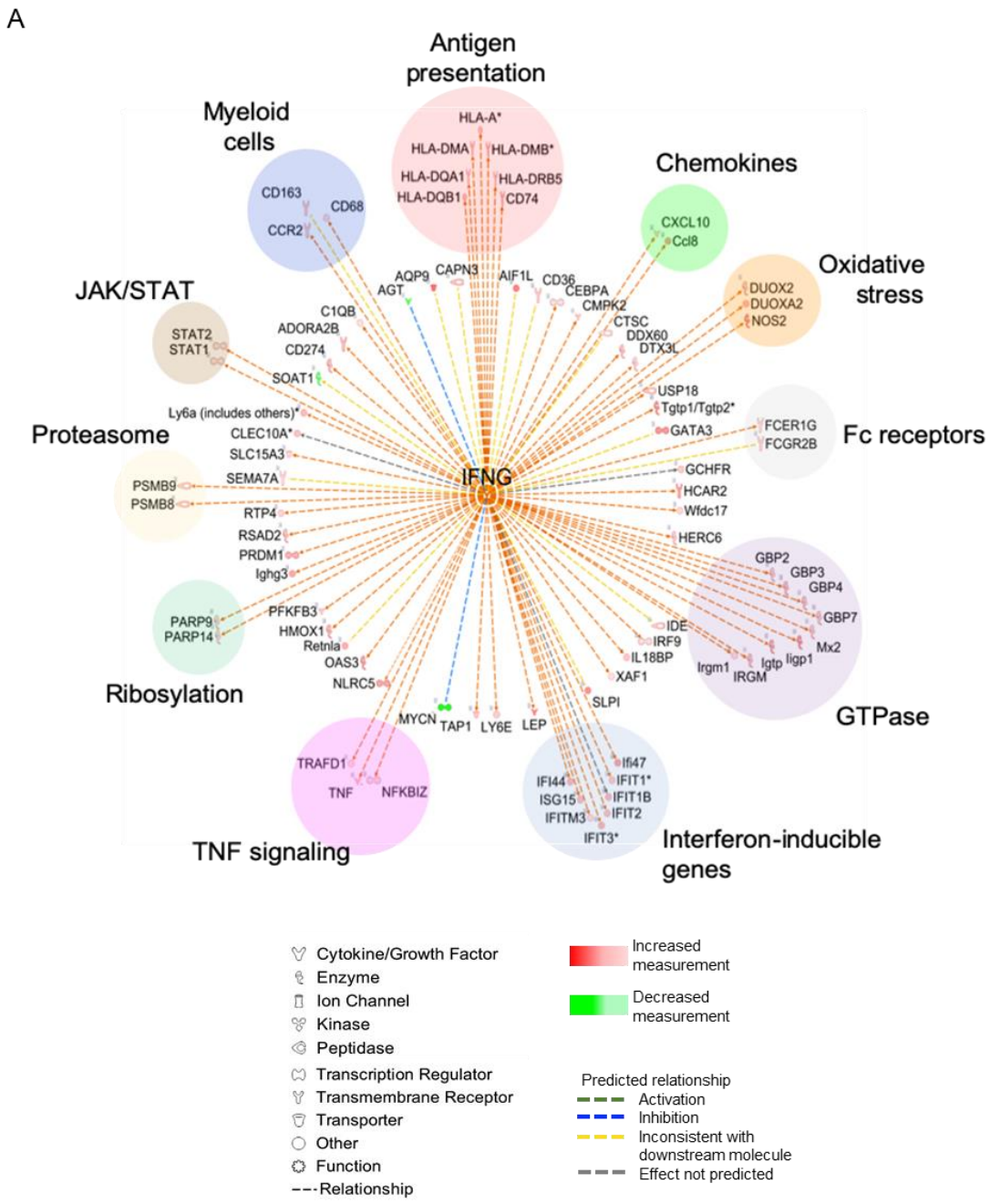

Supplementary Figure 6: Network analysis of *Ifng* interactions with other differentially expressed genes in WT mice following FMT+CPI

(A) Network analysis of annotated *Ifng* interactions with CPI-induced colitis DEGs showed effects on many biological processes, such as antigen presentation, oxidative stress, chemokine induction, JAK/STAT signalling, and proteasome activation.

Supplementary Figure 7

A

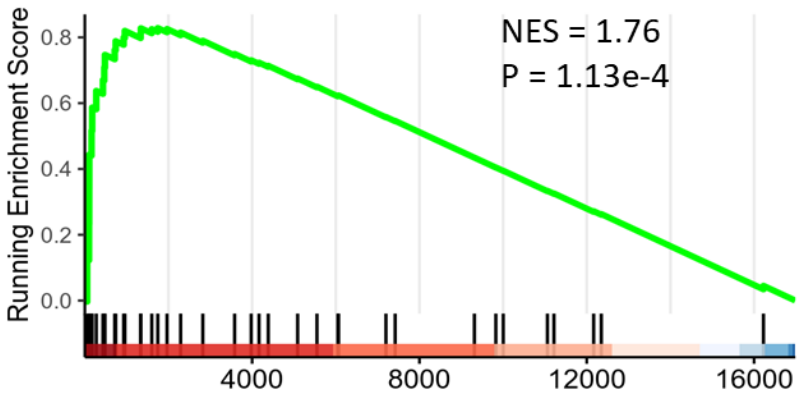

Supplementary Figure 7: Link between transcriptional features of CPI-induced colitis in human and mouse

(A) GSEA results for the mouse homologs of the most significantly up-regulated genes in colon biopsies from patients affected by CPI-induced colitis. 32 human genes significantly up-regulated in CPI-induced colitis (log fold change > 1 and FDR < 0.05) were identified through differential expression analysis of a previously published dataset focusing on the nCounter PanCancer Immune Profiling Panel. The gene signature consisted of all their 39 mouse homologs expressed in WT mice (n=4) and in mice treated with FMT and anti-CTLA4/anti-PD-1 combination therapy (n=3). The mouse genes were ranked based on the estimated expression log fold changes between these conditions, using the control as reference. NES: Normalised Enrichment Score, P: P-value of the gene set enrichment test.

Supplementary Figure 8

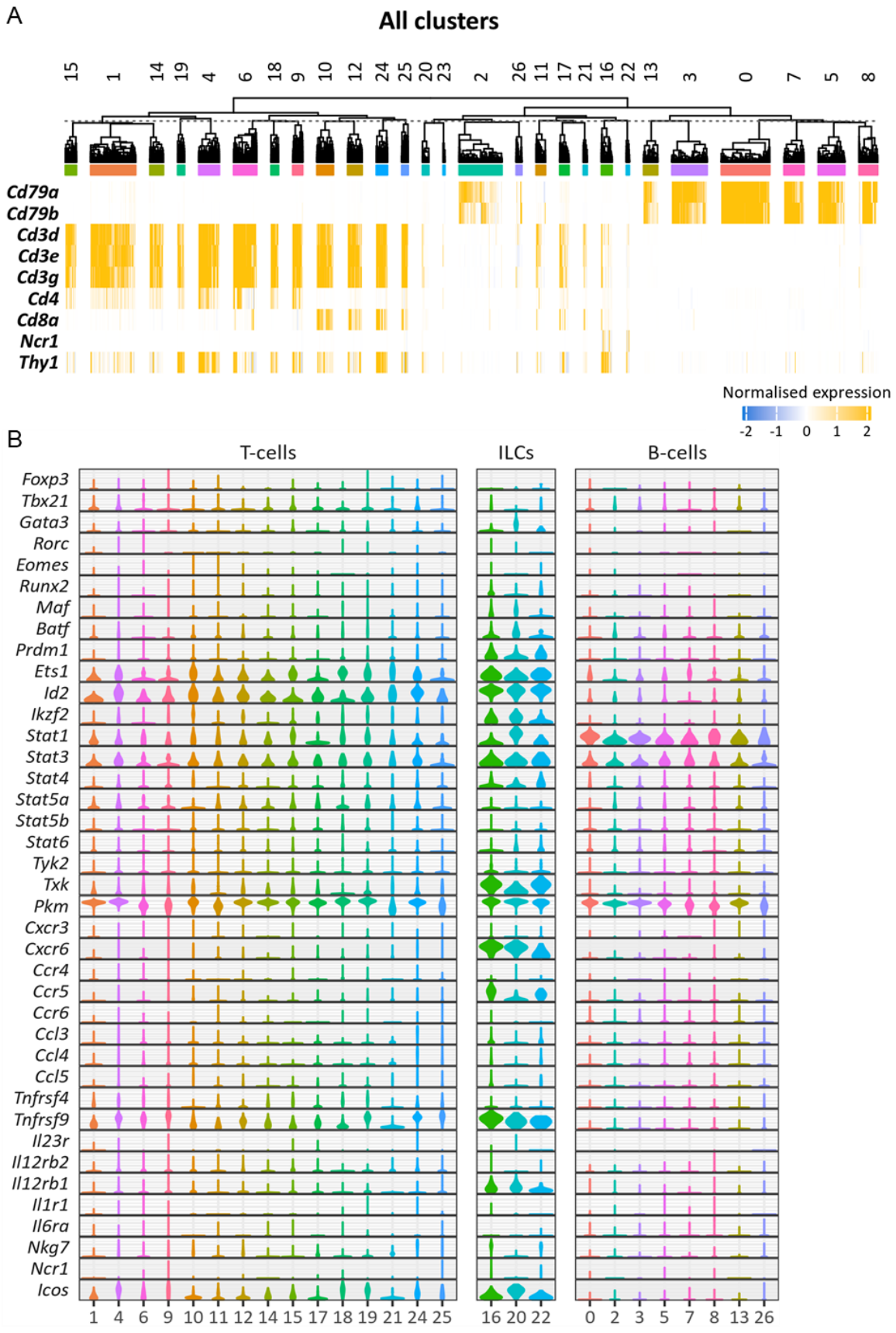

Supplementary Figure 8: Single cell RNA-seq analysis of different immune compartments reveals that IFNγ is a key cytokine in CPI-induced colitis

(A) Heatmap of normalised gene expression levels of different surface markers across the 27 lymphocyte populations identified in the control samples (n=3) used in this study. (B) Violin plots of normalised gene expression levels of different transcription factors, kinases, chemokine receptors and chemokines in the T cells, B cells and ILC clusters.

Supplementary Figure 9

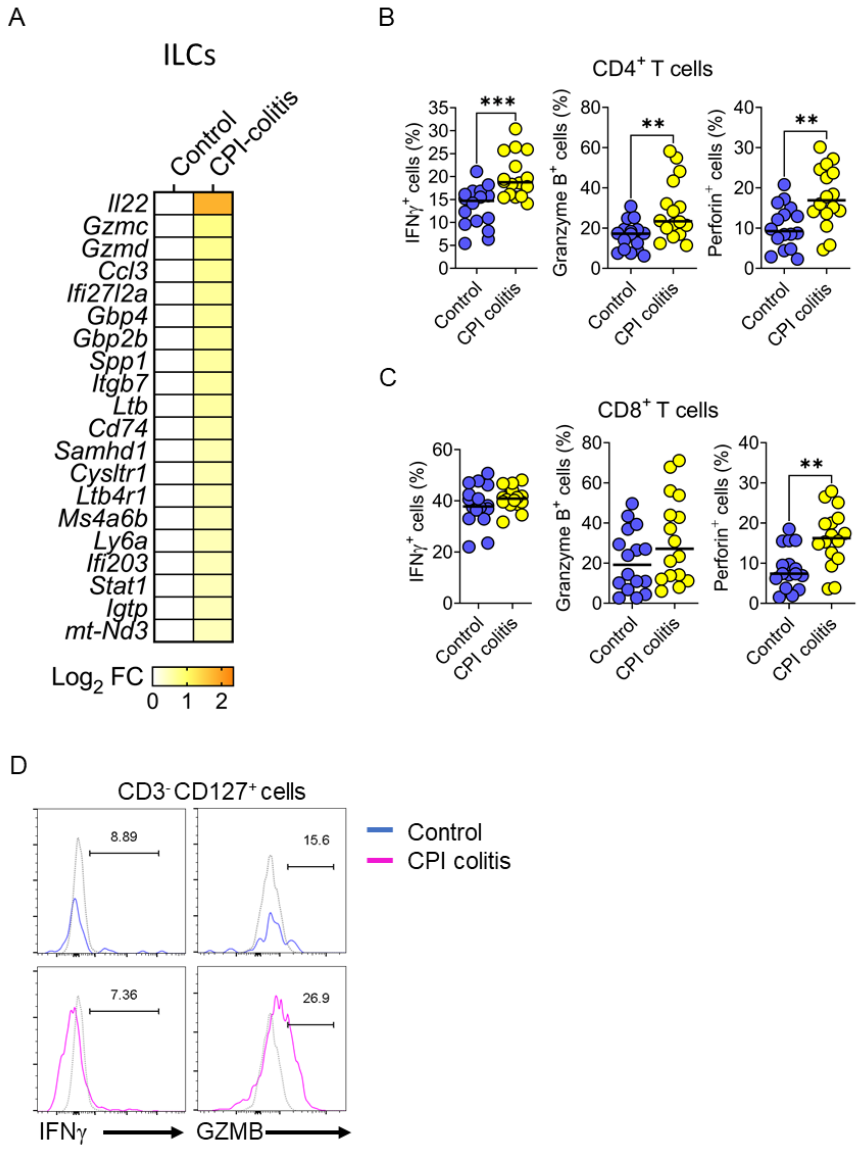

Supplementary Figure 9: Cytotoxic profile by flow cytometry of CD4$^+$ and CD8$^+$ T-cells

(A) Heatmap of cytokine and chemokine expression shown by $\log_2$ fold changes between CPI-induced colitis (n=3) and control samples (n=4) in colonic ILC clusters. (B) Dot plots from flow cytometry data showing the proportions of IFNγ, granzyme B and perforin producing CD4$^+$ and (C) CD8$^+$ T cells in WT mice (n=16) and in mice treated with FMT and CPI (n=16). Representative flow cytometry histograms showing the percentage of IFNγ and granzyme B expressing CD3$^-$ CD127$^+$ cells in mice with CPI-induced colitis (n=16) and control mice (n=16).

Supplementary Figure 10

A

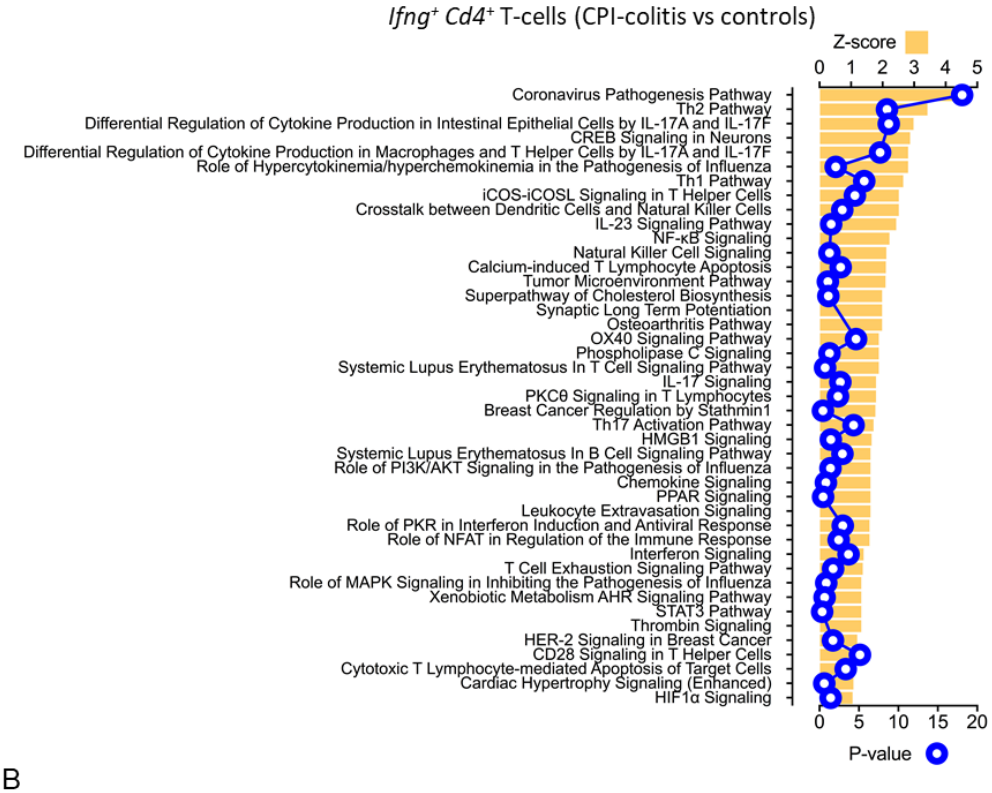

B

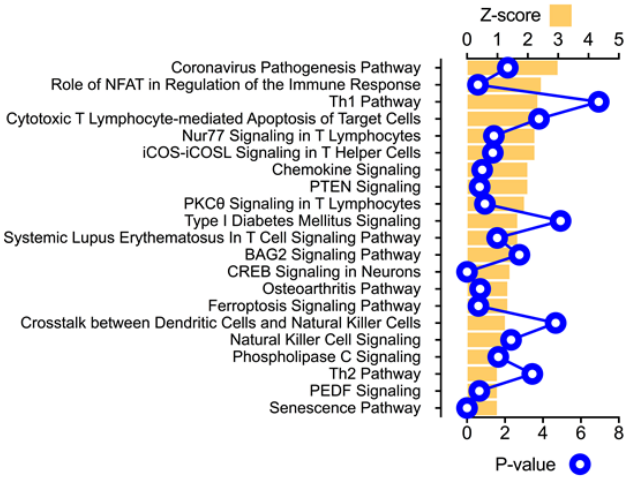

Supplementary Figure 10: Canonical pathways activated in *Ifng*$^+$ CD4$^+$ and CD8$^+$ T cells

(A) Canonical pathways activated (Z-score >1) in *Ifng*$^+$ CD4$^+$ and (B) CD8$^+$ T cells in CPI colitis (n=3) vs controls (n=4).

Supplementary Figure 11

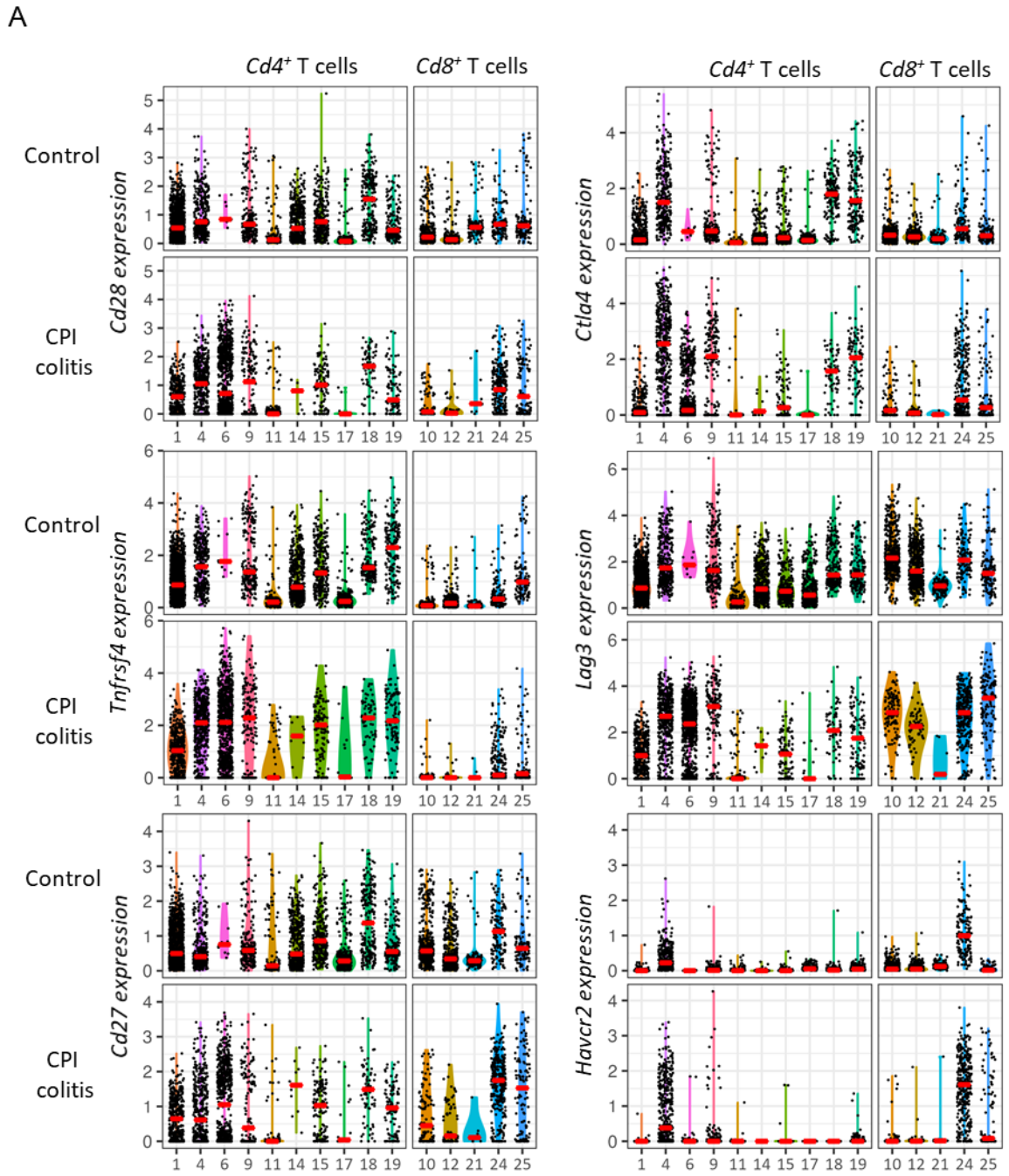

Supplementary Figure 11: Violin plots showing expression of different checkpoint genes in the CD4$^+$ and CD8$^+$ T cell clusters from the single cell RNA-seq dataset

(A) Violin plots showing the expression levels of checkpoint genes across CD4$^+$ and CD8$^+$ T cell clusters in mice with CPI-induced colitis.

Supplementary Figure 12

A

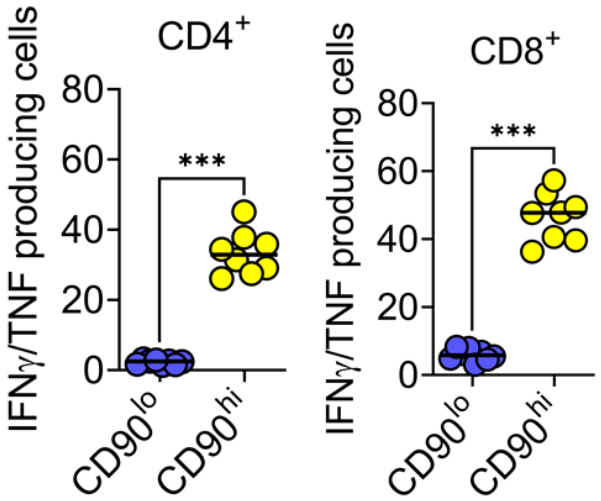

Supplementary Figure 12: CD90^{hi} CD4^{+} and CD8^{+} show increased polyfunctional cytotoxic cytokines in CPI-induced colitis

(A) Summary statistics showing intracellular IFNγ/TNFα in CD4^{+} and CD8^{+} T cells in the colon in mice treated FMT+CPI. Cells were stimulated with PMA/ionomycin *** P< 0.001 two sided Mann-Whitney U test.

Supplementary Figure 13

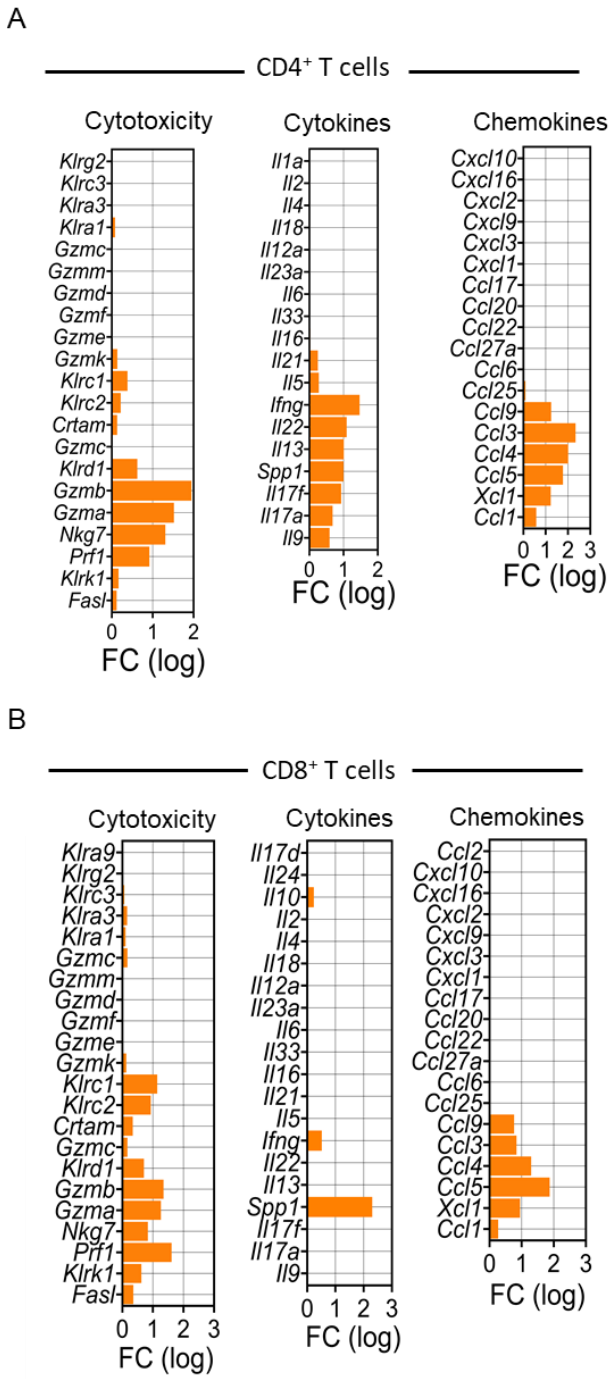

Supplementary Figure 13: IFNγ$^+$ CD4$^+$ and CD8$^+$ T cells have increased expression of cytotoxic genes

(A) Bar graph of expression levels of significantly expressed cytotoxic, cytokines and chemokines genes in IFNγ$^+$ CD4$^+$ T cell clusters and (B) CD8$^+$ T cell clusters compared to IFNγ$^-$ clusters.

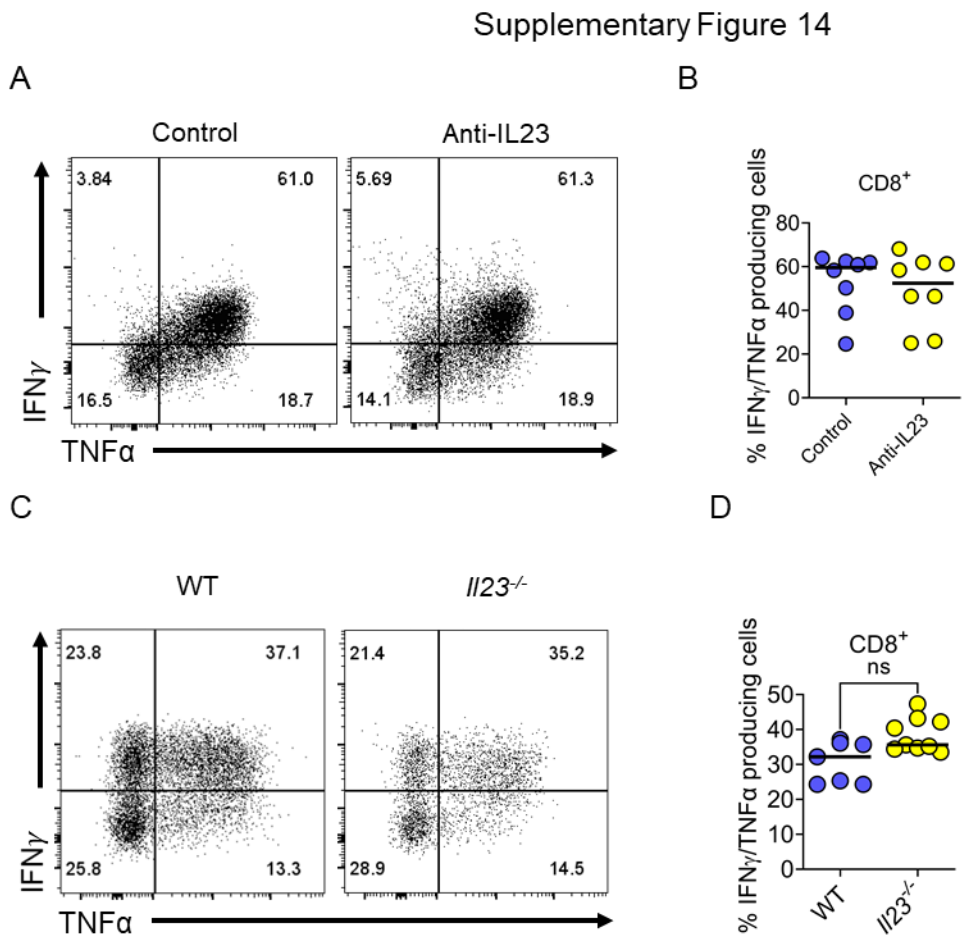

Supplementary Figure 14: CD8$^+$ T cells remain unaffected by blockade or deletion of IL23

(A) Representative flow cytometry plot and (B) percentage of IFNγ$^+$/TNFα$^+$ CD8$^+$ T cells from CPI-colitis mice treated with an isotype control (n=7) or an IL-23 blocking antibody (n=8). (C) Representative flow cytometry plot and (D) percentage of IFNγ$^+$/TNFα$^+$ CD8$^+$ T cells from CPI-colitis treated wildtype mice (n=8) or *Il23*$^{-/-}$ mice (n=12).